Pergamon

Cement and Concrete Research 29 (1999) 855–859

CEMENT AND CONCRETE RESEARCH

Fracture mechanics parameters of autoclaved aerated concrete

B. Trunk [a,*], G. Schober [b], A.K. Helbling [a], F.H. Wittmann [a]

[a] *Institute for Building Materials, Swiss Federal Institute of Technology, CH-8093 Zürich, Switzerland*

[b] *Hebel AG, D-82243 Fürstenfeldbruck, Germany*

Manuscript received 16 January 1998; accepted manuscript 22 February 1999

Abstract

The influence of the expanding direction of Autoclaved Aerated Concrete (AAC) on the nonlinear fracture mechanics parameters is determined on three different types of AAC. The nonlinear fictitious crack model introduced by Hillerborg et al. [1] is used. Based on the RILEM recommendation AAC 13.1 [2], wedge-splitting tests have been carried out on three different types of AAC. For each AAC type, specimens were prepared so that the ligament area was parallel or vertical to the expanding direction. It was found that the specific fracture energy G_f and the tensile strength f_t differ in the two directions. All three concrete types show less brittle behaviour when the ligament area is parallel to the expanding direction.

Keywords: Fracture mechanics; Fictitious crack model; AAC; Ductility; Expanding direction

Until now many fracture mechanics tests have been carried out on AAC (see for example [3,4]). It was found that cracking in AAC can be described with nonlinear fracture mechanics models like the fictitious crack model from Hillerborg et al. [1] in a realistic way. With a slightly modified wedge-splitting test setup based on the RILEM recommendation AAC 13.1 [2], tests have been carried out on AAC specimens in order to study the influence of the direction of expansion on the nonlinear fracture mechanics parameters and the ductility. Three different kinds of AAC have been tested.

1. Experimental procedure

Nonlinear fracture mechanics parameters were obtained by means of the wedge-splitting test [5]. A schematical illustration of the test setup is given in Fig. 1. Two wedges are pressed symmetrically between four roller bearings in order to split the specimen into two halves. The test setup is similar to the RILEM recommendation AAC 13.1 [2] with one difference: the specimen is placed on two line supports, not only on one single line support in the centre of the specimen (see Fig. 2). The supports are right under the mass concentration points of each half specimen. An advantage of this loading arrangement is that a multiaxial stress distribution at the end of the crack path is avoided. A similar experimental arrangement has also been used by Guofan et al. [6] and van Gils et al. [7]. Otherwise, the crack is forced to propagate through the damaged material. This damage certainly will influence the measured fracture energy G_f.

The crack mouth opening displacement (CMOD) at both sides of the specimen immediately under the loading points (see Fig. 1) and the applied vertical load F are measured. From the measured vertical load and the wedge angle the horizontal splitting force is calculated. The measured CMOD is the mean value of the two displacement transducers on the two opposite sides of the specimen. All tests were run under CMOD control. The rate of CMOD was 60 μm/s.

The work of fracture is calculated from the area under the splitting force CMOD diagram. The specific fracture energy G_f is the work of fracture divided by the ligament area A_{lig}. The ligament area A_{lig} is the projected area on a plane parallel to the ideal crack direction; in other words, the ligament height multiplied by the specimen thickness.

To determine the nonlinear fracture mechanics parameters from all experimental results of one series, a mean load deflection diagram is calculated as described by Brühwiler [8]. With an inverse analysis based on finite element calculations as described by Roelfsta and Wittmann [9], the bilinear approximated strain-softening diagram is obtained. The nonlinear finite element program SOFTFIT initially implemented by Roelfstra [10] is used. In Fig. 3 an example of a

* Corresponding author. B. Trunk is now at DaimlerChrysler AG, Eyachstr. 34, 71065 Sindelfingen, Germany. Tel.: 49-7031-90-88-961; Fax: 49-7031-90-82-773; E-mail: bernhard.trunk@ daimlerchrysler.com.

0008-8846/99/$–see front matter
PII: S0008-8846(99)00059-9

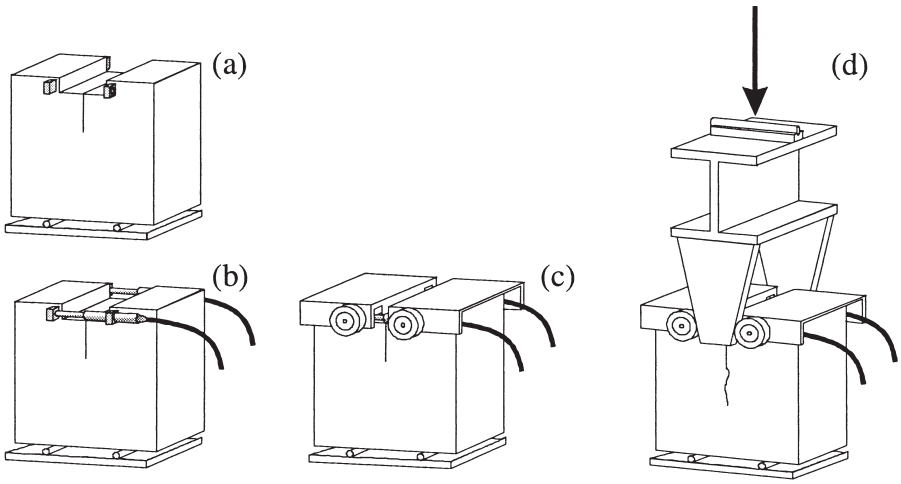

Fig. 1. Principle of the wedge-splitting test: *(a)* specimen on two linear supports, *(b)* displacement transducers on both sides of the specimen, *(c)* steel loading devices with roller bearings, *(d)* traverse with wedges.

bilinear approximated strain-softening diagram with all significant parameters is given. The specific fracture energy G_f is equal to the area under the strain-softening curve.

The modulus of elasticity E for each AAC type and ligament direction has been calculated from the initial slope of the load deflection curves.

2. Preparation of specimens

All tested specimens had the same dimensions and these are given in Fig. 4. The dimensions were the same as recommended by RILEM AAC 13.1 [2]. The specimens were sawed from bigger blocks and stored under constant climatic conditions of 60% relative humidity and 20°C. For each type of AAC and each direction, six specimens were tested.

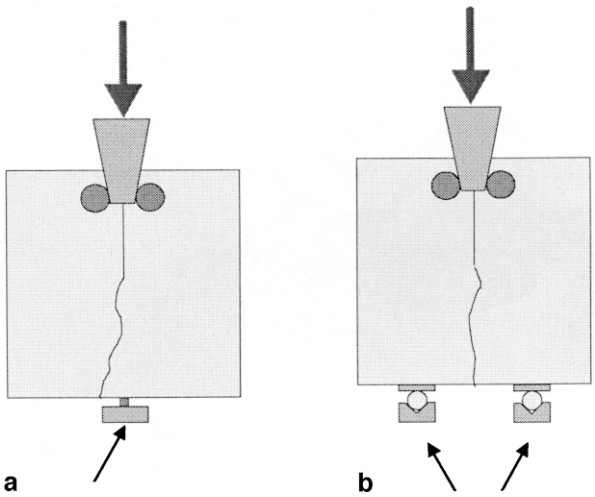

Fig. 2. Modified wedge-splitting test setup according to RILEM: AAC 13.1 [2]. *(a)* One single line support at the end of the theoretical crack path. *(b)* Two line supports under the mass concentration points under each half specimen.

After performing the wedge-splitting tests the density ρ and water content w were determined. For this purpose, the tested wedge-splitting specimens were sawed into pieces of 150 × 100 × 50 mm and stored at 105°C until constant weight. The results are summarized in Table 1.

In Table 2 the experimental results are summarized. The numerical specific fracture energy G_f^{num} is determined from the area under the strain-softening diagram. The experimental specific fracture energy G_f^{exp} is determined from the work of fracture and the nominal ligament area as described above. In Fig. 5 the experimental and calculated load deflection curves are given. From Fig. 5 and from the agreement between the numerical and experimental specific fracture energy it can be seen that there is a good agreement between the bilinear approximated strain-softening curve and the experimental results. It can be assumed that the bilinear approximation of the strain-softening behaviour is realistic to describe crack formation and propagation in AAC. In Fig. 6 the bilinear approximated strain-softening relations are illustrated.

It can be seen that for all three AAC types the fracture energy G_f of the specimens with the ligament area parallel to the expanding direction is higher than when vertical to it. In contrast to this fact, the tensile strength of the specimens with the ligament in the vertical direction is higher than in the expanding direction. Except for AAC type A2 the modulus of elasticity is independent of the expanding direction. The Young's modulus of AAC type A2 differs slightly only within the experimental scatter in the two tested directions.

3. Evaluation of results

In order to characterize the ductility of a material, Petersson [11] and Hillerborg [12] introduced the characteristic length l_{ch} [Eq. (1)]:

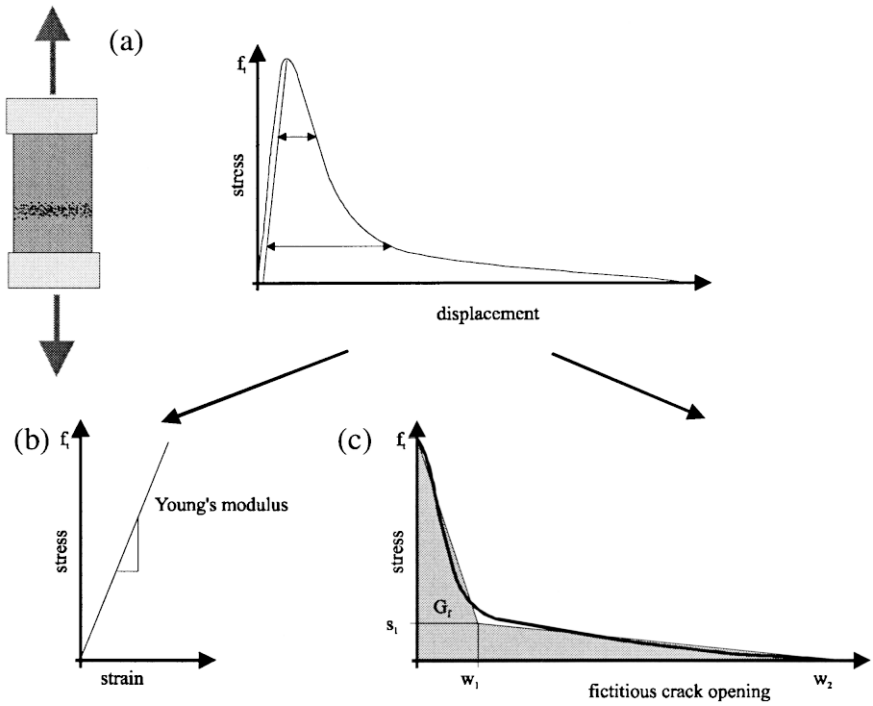

Fig. 3. Parameters of the bilinear approximated strain-softening relation: *(a)* stress displacement curve for a direct tension test; *(b)* linear elastic material behaviour, before the tensile strength is reached; *(c)* strain-softening relation with a bilinear approximation.

$$l_{ch} = \frac{E \cdot G_f}{f_t^2} \tag{1}$$

The characteristic length l_{ch} does not take the slope of the strain softening diagram into consideration and for that reason it is essentially a technological quantity. Materials with a similar strain-softening behaviour can be compared. The smaller the characteristic length l_{ch} the more brittle and the less resistant against cracking is the material. So it can be seen that a high tensile strength f_t leads to more brittle material behaviour. On the other hand, a high value of the Young's modulus E or a high specific fracture energy G_f will cause a more ductile behaviour.

Another possibility to characterise the ductility of a material is to take the steepest slope of the strain-softening diagram into consideration. This leads to the following formulation for a critical specimen length l_{crit} under direct tension [11,13] [Eq. (2)]:

$$l_{crit} = \left.\frac{\partial \sigma(w)}{\partial w}\right|_{\min} = \frac{f_t - s_1}{w_1} \tag{2}$$

In Table 2 the characteristic and critical lengths l_{ch} and l_{crit} for each AAC type and ligament direction are given. Both the characteristic and critical lengths l_{ch} and l_{crit} show that all three AAC types are less brittle when the ligament area is parallel to the direction of expansion.

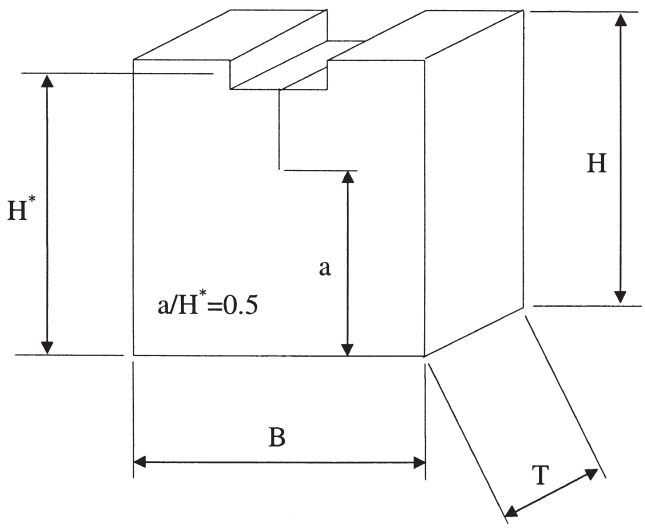

Fig. 4. Dimensions of the wedge-splitting specimens. H = 200 mm, H* = 185 mm, B = 200 mm, a = 97.5 mm, T = 100 mm.

4. Conclusions

From the test results obtained on all three types of AAC it can be seen that the direction of expansion has a signifi-

Table 1
Density and water content of the three types of AAC tested

Type	Density ρ (kg/m^3)	Water content w (%)
A1	398.3	4.3
A2	413.7	4.4
A3	397.5	4.1

Table 2
Fracture mechanical parameters

Type	E (N/mm^2)	G_f^{exp} (N/m)	G_f^{num} (N/m)	f_t (N/mm^2)	s_1 (N/mm^2)	w_1 (mm)	w_2 (mm)	l_{ch} (mm)	l_{crit} (mm)
A1									
∥	1300	6.234	6.3	0.272	0.089	0.02	0.080	109.5	142.3
⊥	1300	5.984	5.9	0.304	0.070	0.02	0.080	84.2	111.3
A2									
∥	1500	6.516	6.7	0.314	0.090	0.02	0.080	99.13	134.2
⊥	1400	6.336	6.15	0.326	0.068	0.02	0.085	83.5	108.5
A3									
∥	1500	6.195	6.5	0.368	0.036	0.03	0.085	68.6	124.1
⊥	1500	5.614	6.1	0.377	0.057	0.02	0.080	59.2	93.8

cant influence on the ductility of AAC. The specific fracture energy G_f is higher and the tensile strength f_t is lower when measured parallel to the expanding direction. The maximum splitting force, which is caused by the tensile strength f_t, the strain softening behaviour $\sigma(w)$, and the fracture energy G_f show the same tendency as the fracture energy G_f. There is no significant influence of direction of testing on the modulus of elasticity E. The characteristic and critical lengths l_{ch} and l_{crit} show that all three types of AAC are less brittle when tested parallel to the expanding direction as compared to the normal direction. From Table 2 it can also be seen that ductility of the three types of AAC vary considerably. While type A1 can be considered to be comparatively ductile, type A3 is much more brittle.

References

[1] A. Hillerborg, M. Modeer, P.E. Pettersson, Analysis of crack formation and crack growth in concrete by means of fracture mechanics and finite elements, Ceme Concr Res 6 (1976) 773–782.
[2] RILEM Recommendation AAC13.1, Determination of the specific fracture energy and strain softening of AAC, RILEM Technical Rec-

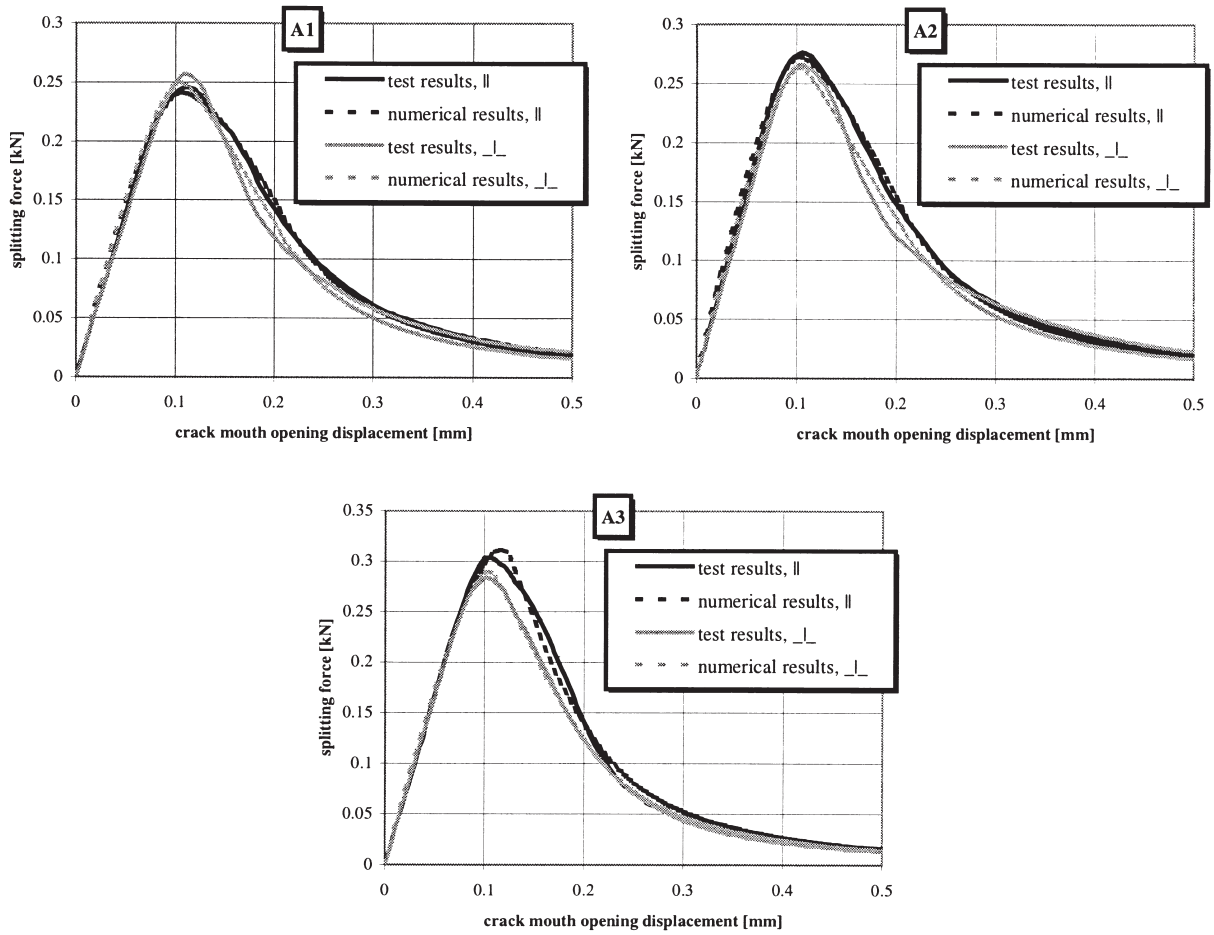

Fig. 5. Test results and numerical simulation.

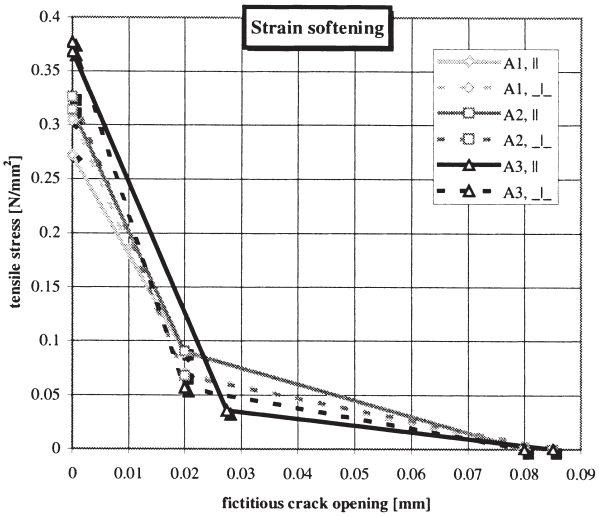

Fig. 6. Bilinear approximated strain-softening relations for each test series.

ommendations for the testing and use of construction materials, E & FN Spon, 1994, pp. 156–158.

[3] E. Brühwiler, J. Wang, F.H. Wittmann, Fracture of AAC as influenced by specimen dimension and moisture, Journal of Materials in Civil Engineering 2 (3) (1990) 136–146.

[4] V. Slowik, F.H. Wittmann, Fracture energy and strain softening of AAC, in: Advances in autoclaved and aerated concrete, F.H. Wittmann (ed.), Balkema, Rotterdam and Brookfield, 1992, pp. 141–145.

[5] E. Brühwiler, F.H. Wittmann, The wedge splitting test, a method of performing stable fracture mechanics tests, Engineering Fracture Mechanics 35 (1990) 117–126.

[6] Z. Guofan, J. Hui, X. Shilang, Study of fracture toughness and fracture energy by means of wedge splitting test specimens, in: Brittle Matrix Composites, A.M. Brand, I.H. Marshall (eds.), Elsevier Applied Science, London and New York, 1991, pp. 62–71.

[7] M.A.J. Gils van, L.J.M.G. Dortmans, G. de With, Fictitious crack modelling of Kiln furniture ceramics, in: Fracture mechanics of concrete structures, F.H. Wittmann (ed.), Aedificatio Publishers, Freiburg, Germany, 1995, pp. 1261–1270.

[8] E. Brühwiler, Bruchmechanik von Staumauerbeton unter quasi-statischer und erdbebendynamischer Belastung, PhD Thesis, École Polytechnique Fédérale de Lausanne, Switzerland, 1988.

[9] P.E. Roelfstra, F.H. Wittmann, Numerical method to link strain softening with failure of concrete, in: Fracture Toughness and Fracture Energy of Concrete, F.H. Wittmann (ed.), Elsevier Science, Amsterdam, 1986, pp. 163–175.

[10] P.E. Roelfstra, A numerical approach to investigate the properties of concrete numerical concrete, PhD Thesis, École Polytechnique Fédérale de Lausanne, Switzerland, 1989.

[11] P.E. Petersson, Crack growth and development of fracture zones in plain concrete and similar materials, Report TVBM-1006, Lund Institute of Technology, Lund, Sweden, 1981.

[12] A. Hillerborg, Analysis of one single crack, in: Fracture Mechanics of Concrete, F.H. Wittmann (ed.), Elsevier Science, Amsterdam, 1983, pp. 223–294.

[13] B. Trunk, H. Sadouki, F.H. Wittmann, Size effect and stability of fracture, in: Fracture mechanics of concrete structures, F.H. Wittmann (ed.), Aedificatio Publishers, Freiburg, Germany, 1995, pp. 607–618.